Stability, Power Sharing, & Distributed Secondary Control in Droop-Controlled Microgrids

John W. Simpson-Porco, Florian Dörfler, Francesco Bullo
Center for Control, Dynamical Systems and Computation
University of California at Santa Barbara
Santa Barbara, California 93106
Email: johnwsimpsonporco@engineering.ucsb.edu

Qobad Shafiee, Josep M. Guerrero
Institute of Energy Technology
Aalborg University
Aalborg East DK-9220, Denmark
Email: qsh@et.aau.dk

***Abstract*—Motivated by the recent and growing interest in microgrids, we study the operation of droop-controlled DC/AC inverters in an islanded microgrid. We present a necessary and sufficient condition for the existence of a synchronized steady state that is unique and locally exponentially stable. We discuss a selection of controller gains which leads to a sharing of power among the generators, show that this proportional selection enforces actuation constraints for the inverters. Moreover, we propose a distributed integral controller based on averaging algorithms which dynamically regulates the system frequency in the presence of a time-varying load. Remarkably, this distributed-averaging integral controller has the additional property that it maintains the power sharing properties of the primary droop controller. Finally, we present experimental results validating our controller design, along with simulations of extended scenarios. Our results hold without assumptions on uniform line admittances or voltage magnitudes.**

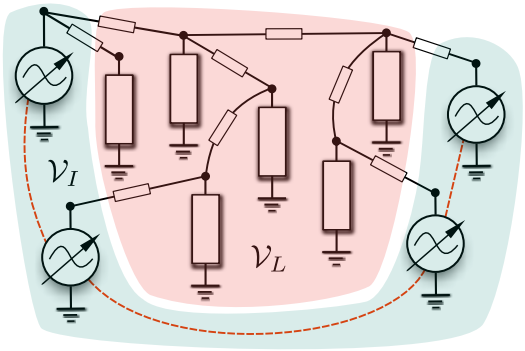

Fig. 1. Schematic illustration of a microgrid, with four inverters (nodes $\mathcal{V}_I$) supplying six loads (nodes $\mathcal{V}_L$) through an acyclic interconnection. The dotted lines between inverters represent communication links, which will be used exclusively in Section VI for secondary control.

I. Introduction

Microgrids are low-voltage electrical distribution networks, heterogeneously composed of distributed generation, storage, load, and managed autonomously from the larger primary network. Microgrids are able to connect to the wide area electric power system through a Point of Common Coupling (PCC), but are also able to "island" themselves and operate independently [1]. Energy generation within a microgrid can be highly heterogeneous, including photovoltaic, wind, geothermal, micro-turbines, etc. Many of these sources generate either variable frequency AC power or DC power, and are interfaced with a synchronous AC grid via power electronic DC/AC *inverters*. In islanded operation, it is through these inverters that actions must be taken to ensure synchronization, security, power balance and load sharing in the network [2].

Inspired by control architectures from transmission level power systems, control in microgrids is generally approached in a hierarchical manner [1]. The first and most basic level is *primary* control, which is concerned with the stability of — and load sharing within — the electrical network. Although centralized architectures have been used for primary control, in order to enhance redundancy and enable "plug-and-play" functionality the standard is to employ decentralized proportional control loops locally at each inverter [2]–[7]. While generally successful, these decentralized "droop" controllers typically force both the local voltages and the steady-state network frequency to deviate from their nominal values.

This leads naturally to the next level in the control hierarchy, termed *secondary* control. Generally speaking, the goal of secondary control is to remove the aforementioned deviations in both global frequency and local voltage. Centralized techniques for secondary control have been well studied in classical wide-area transmission and distribution networks, see [8]. These centralized strategies have also been applied in the context of microgrids, and the term "secondary" has been broadened to include additional control goals such as harmonic compensation and voltage unbalance, see [1], [2], [9], [10] for various works.

In this work we present recent theoretical and experimental results on primary and secondary control in microgrids [11]. After a review of the droop control method and secondary control (Section II), we provide necessary and sufficient conditions for the existence of a stable operating point for a network of droop-controlled inverters and loads (Section III–IV), and rigorously establish control parameter selections and bounds on loads which result in the inverters meeting given actuation constraints (Section V). In Section VI we propose a novel distributed secondary controller, based on Laplacian averaging algorithms, which quickly regulates the network frequency to a nominal value. Remarkably, this controller accomplishes this task while maintaining the power sharing properties of the primary droop controller. In Sections VII and VIII we provide

experimental and simulation results validating our controller designs, before offering conclusions and future directions in Section IX. Detailed proofs of all results can be found in [11].

II. Review of Distributed Control in Microgrids

A. Problem Setup and Review of Circuit Theory

In this work we model an AC microgrid by a connected, undirected, and complex-weighted graph with nodes (or buses) $\mathcal{V} = \{1, \dots, n\}$, edges (or branches) $\mathcal{E} \subset \mathcal{V} \times \mathcal{V}$, and symmetric edge weights (or admittances) $-Y_{ij} = -Y_{ji} \in \mathbb{C}$ for every branch $\{i, j\} \in \mathcal{E}$. We partition the set of buses as $\mathcal{V} = \mathcal{V}_L \cup \mathcal{V}_I$, corresponding to the loads and inverters. To each bus $i \in \mathcal{V}$, we associate a complex power injection $S_i = P_i + jQ_i$ and the phasor voltage variable $E_i e^{j\theta_i}$ corresponding to the magnitude and the phase shift of a solution to the AC power flow equations. For inductive lines, the power flow equations are

$$P_i = \sum\nolimits_{j=1}^{n} \mathrm{Im}(Y_{ij}) E_i E_j \sin(\theta_i - \theta_j), \qquad i \in \mathcal{V}, \quad \text{(1a)}$$

$$Q_i = -\sum\nolimits_{j=1}^{n} \mathrm{Im}(Y_{ij}) E_i E_j \cos(\theta_i - \theta_j), \quad i \in \mathcal{V}. \quad \text{(1b)}$$

If a number ℓ and an arbitrary direction is assigned to each branch $\{i, j\} \in \mathcal{E}$, the *incidence matrix* A is defined component-wise as $A_{k\ell} = 1$ if bus k is the sink bus of branch ℓ and as $A_{k\ell} = -1$ if bus k is the source bus of branch ℓ, with all other elements being zero. In the inductive network case, for every set of balanced power injections P_i there exists a branch vector ξ satisfying Kirchoff's Current Law (KCL) $P = A\xi$ [12]. For tree networks such as distribution networks, ξ is unique and is given by $\xi = (A^T A)^{-1} A^T P$ [13]. The vector P is interpreted as bus injections, with ξ being the associated branch flows. We denote by ξ_{ij} the component of the branch-vector ξ corresponding to the branch $\{i, j\} \in \mathcal{E}$.

As is standard in the microgrid literature, we model an inverter as a controllable voltage source behind a reactance. This model is widely adopted among experimentalists in the microgrid field. Further modeling explanation can be found in [14]–[16] and the references therein.

B. Review of Primary Droop Control

The *conventional droop controller* is the foundational technique for primary control (synchronization and power balancing) in islanded microgrids, and is a heuristic based on the classic active/reactive decoupling assumption for small power angles and non-mixed line conditions, see [1]–[3], [5], [6], [9], [17]–[21]. For the case of inductive lines, the droop method specifies both the inverter frequencies ω_i and voltage magnitudes E_i by

$$\omega_i = \omega^* - m_i(P_i - P_i^*), \quad i \in \mathcal{V}_I, \quad \text{(2a)}$$

$$E_i = E_i^* - n_i(Q_i - Q_i^*), \quad i \in \mathcal{V}_I, \quad \text{(2b)}$$

where ω^* is a nominal network frequency, E_i^* (resp. P_i^*, Q_i^*) is the *nominal* voltage set point (resp. nominal active/reactive power injection) for the i^{th} inverter, and P_i (resp. Q_i) is the *measured* active (resp. reactive) power injection. The controller gains $m_i, n_i > 0$ are referred to as droop coefficients.

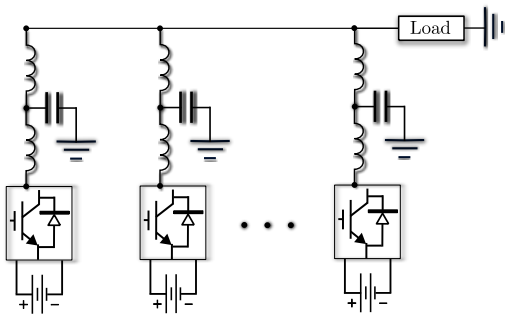

Fig. 2. Schematic of inverters operating in parallel.

In islanded operation, one typically sets $P_i^* = Q_i^* = 0$. From (2a), it is clear that if an inverter injects an amount of power P_i which differs from its pre-determined nominal injection P_i^*, its frequency will deviate from ω^*. While small signal stability analysis of (2a) is standard, in this work we present large-signal results specifying when a steady-state is feasible for the network.

C. Review of Classical Secondary Control

The removal of the steady state frequency deviation generated by the droop controller is accomplished by so-called "secondary" integral controllers. If the primary controller stabilizes the network, then the frequency of each inverter has converged to a steady state value ω_{ss}, and a slower additional control loop can then be used locally at each inverter [9]. Each local secondary controller slowly modifies the controller gain P_i^* until the frequency deviation is zero. This procedure implicitly assumes that the measured local frequency is a good approximation of the steady state network frequency, and relies on a *separation of time-scales* between the fast, synchronization-enforcing primary droop controller and the slower, secondary integral controller [7], [9], [10]. For small droop coefficients m_i, this approach can be particularly slow, leading to an inability of the method to dynamically regulate the network frequency in the presence of a time-varying load. Moreover, these decentralized (i.e., local) secondary controllers may destroy the power sharing properties established by the primary droop controller.

Alternatively, a centralized microgrid controller may be used to perform secondary actions. This has the obvious disadvantage of introducing a single point of failure in the system, and may induce communications over prohibitively large distance.

III. Stability Results for Primary Controller

While the inverters are controlled according to the $P - \omega$ droop method (2a) with P_i given by (1a), the constant power loads P_i^* at load buses $i \in \mathcal{V}_L$ must satisfy the power balance relations

$$0 = P_i^* - \sum\nolimits_{j=1}^{n} |Y_{ij}| E_i E_j \sin(\theta_i - \theta_j), \quad i \in \mathcal{V}_L. \quad \text{(3)}$$

Together, equations (2a) and (3) constitute the model for the network. A natural question now arises: under what conditions

on the loads, nominal power injections, network topology, admittances, and droop coefficients is the network stable? The following result provides the definitive answer for general tree networks. This class of networks includes the standard parallel microgrid topology (Figure 2), and most distribution networks after islanding events.

For simplicity in stating our results, we define the vector of loads and nominal power injections $P^* := (P_1^*, \dots, P_n^*)$, the diagonal matrix of inverse droop coefficients $M^\dagger := \mathrm{diag}(0, \dots, 0, m_1^{-1}, \dots, m_{|\mathcal{V}_I|}^{-1})$, and we let $\mathbf{1}_n$ be the n-dimensional vector where each entry is equal to one.

Theorem 1. (Existence and Stability of Sync'd Solution). *Consider the frequency-droop controlled system* (2a) *with loads* (3)*. Define the steady state network frequency* $\omega_{\rm ss}$ *by*

$$\omega_{\rm ss} := \omega^* + \frac{\sum_{i=1}^n P_i^*}{\sum_{i \in \mathcal{V}_I} m_i^{-1}} \,,$$

and let ξ *be the unique vector of branch active power flows, satisfying KCL, namely* $P^* - (\omega_{\rm ss} - \omega^*) M^\dagger \mathbf{1}_n = A\xi$*. The following two statements are equivalent:*

(i) **Synchronization:** *There is a number* $0 \le \gamma < \pi/2$ *such that the closed-loop system* (2a)–(3) *possess a locally exponentially stable and unique synchronized solution* $\theta^*(t)$ *with* $|\theta_i^* - \theta_j^*| \le \gamma$ *for all branches* $\{i,j\} \in \mathcal{E}$*;*

(ii) **Flow Feasibility:** *The active power flow is feasible, i.e.,*

$$\Gamma := \max_{\{i,j\} \in \mathcal{E}} \left| \frac{\xi_{ij}}{E_i E_j |Y_{ij}|} \right| < 1 \tag{4}$$

The parameter Γ *and the angular spread* γ *are then related uniquely via* $\Gamma = \sin(\gamma)$*, the network synchronizes to steady state frequency* $\omega_{\rm ss}$*, and the power angles satisfy* $\sin(\theta_i^* - \theta_j^*) = \xi_{ij}/E_i E_j |Y_{ij}|$ *for each branch* $\{i,j\} \in \mathcal{E}$*.*

Proof: See [11] for all proofs. ∎

As outlined in [11], physically the parametric condition (4) is the very mild stipulation that the active power flow along each branch be feasible, i.e., less than the physical maximum $\xi_{ij,\max} := E_i E_j |Y_{ij}|$. The quantity Γ can therefore be used for monitoring as an indicator of *network stress*. If $\Gamma \simeq 1$, the network is close to collapsing, while if $\Gamma \simeq 0$, safe operation is assured. In practice, thermal constraints may place an upper bound of $\Gamma \simeq 0.25$ or roughly $\max_{(ij) \in \mathcal{E}} |\theta_i - \theta_j| \simeq 15^\circ$.

IV. Robustness to Voltage Dynamics

The analysis so far has been based on the assumption that the product $E_i E_j |Y_{ij}|$ is a *constant and known* parameter for all branches $\{i,j\} \in \mathcal{E}$. In a realistic power system, both effective line susceptances and voltage magnitudes are only approximately known, and are dynamically adjusted by additional controllers, such as the $Q-E$ droop controller (2b). The following result states that as long as these additional controllers can regulate the effective susceptances and nodal voltages above prespecified lower bounds, the stability results of Theorem 1 go through with little modification.

Corollary 2. (Robustified Stability Condition). *Consider the frequency-droop controlled system* (2a) *with loads* (3)*. Assume that the bus voltage magnitudes and branch susceptance magnitudes are above a lower bound. That is, they satisfy* $E_i > \underline{E}_i > 0$ *for all buses* $i \in \{1, \dots, n\}$*, and* $|Y_{ij}| \ge |\underline{Y}_{ij}| > 0$ *for all* $\{i,j\} \in \mathcal{E}$*. The following two statements are equivalent:*

(i) **Robust Synchronization:** *For all possible voltage magnitudes* $E_i > \underline{E}_i$ *and line susceptances* $|Y_{ij}| \ge |\underline{Y}_{ij}|$*, there exists a number* $0 \le \gamma < \pi/2$ *such that the closed-loop system* (2a) *with loads* (3) *possess a locally exponentially stable and unique synchronized solution* $\theta^*(t)$ *with* $|\theta_i^* - \theta_j^*| \le \gamma$ *for all branches* $\{i,j\} \in \mathcal{E}$*;*

(ii) **Worst Case Flow Feasibility:** *The active power flow is feasible for the worst case voltage magnitudes and line susceptances, that is,*

$$\max_{\{i,j\} \in \mathcal{E}} \left| \frac{\xi_{ij}}{\underline{E}_i \underline{E}_j |\underline{Y}_{ij}|} \right| < 1 \,. \tag{5}$$

V. Power Sharing and Power Injection Limits

While Theorem 1 addresses the concern of stability for the frequency-droop controlled system (2a) with loads (3), it does not take into account that the inverter power injections must satisfy *actuation constraints*. That is, we must have $0 \le P_i \le \overline{P}_i$ for some $\overline{P}_i > 0$ called the *rating* of inverter i. The following definition gives the proper criteria for selection.

Definition 1. (Proportional Droop Coefficients). *The droop coefficients are selected proportionally if* $m_i P_i^* = m_j P_j^*$ *and* $P_i^*/\overline{P}_i = P_j^*/\overline{P}_j$ *for all* $i, j \in \mathcal{V}_I$*.*

While the first condition in Definition 1 is standard in the microgrid literature, the second is a generalization of the choice $P_i^* = \overline{P}_i$. The next result shows that this proportional selection leads to desirable steady state power injections.

Theorem 3. (Power Flow Constraints and Power Sharing). *Consider a synchronized solution of the frequency-droop controlled system* (2a) *with loads* (3)*, and let the droop coefficients be selected proportionally. Define the total load* $P_L := \sum_{i \in \mathcal{V}_L} P_i^*$*. The following two statements are equivalent:*

(i) **Injection Constraints:** $0 \le P_i \le \overline{P}_i, \quad \forall i \in \mathcal{V}_I$*;*

(ii) **Load Constraint:** $-\sum_{j \in \mathcal{V}_I} \overline{P}_j \le P_L \le 0$*.*

Moreover, the inverters share the total load P_L *proportionally according to their power ratings, that is,* $P_i/\overline{P}_i = P_j/\overline{P}_j$ *for each* $i, j \in \mathcal{V}_I$*.*

In particular, note that the implication (ii)⇒(i) of Theorem 3 shows that if the total load is feasible for the inverters to service, then Theorem 3 guarantees that *every* inverter satisfies its actuation constraint. Also, for any load P_L satisfying Theorem 3 (ii), we can combine the expression for $\omega_{\rm ss}$ from Theorem 1 with the bounds in Theorem 3 (ii) to calculate that $0 \le \omega_{\rm ss} - \omega^* \le \Delta\omega_{\max} := m_i P_i^*$. W We therefore obtain the classic selection of droop coefficients $m_i = P_i^*/\Delta\omega_{\max}$, where $\Delta\omega_{\max}$ is selected to be, say, $(2\pi \cdot 0.1)$Hz [21].

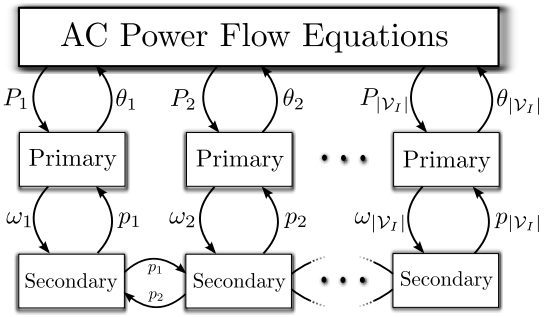

Fig. 3. Schematic of DAPI control architecture.

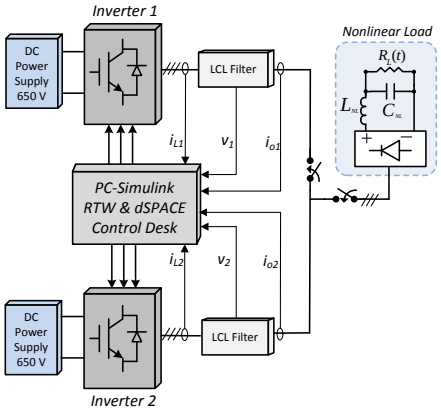

Fig. 4. Schematic illustration of experimental setup.

VI. A Novel Distributed Secondary Controller using Averaging

As is evident from the expression for the steady state frequency $\omega_{\rm ss}$ in Theorem 1, the frequency-droop method almost always leads to a deviation of the steady state operating frequency from the nominal value ω^*.

In what follows, we pursue a scheme for frequency restoration which does not implicitly rely on a separation of time-scales as in [7], [9], [10]. Assuming the existence of a sparse communication network among the inverters, we expand on the conventional frequency-droop design (2a) and propose the *distributed-averaging proportional-integral (DAPI) controller*

$$\omega_i = \omega^* - m_i(P_i - P_i^* + p_i)\,, \tag{6a}$$

$$k_i \frac{\mathrm{d}p_i}{\mathrm{d}t} = \omega_i - \omega^* + \sum_{j\in\mathcal{V}_I} L_{ij}\left(m_i p_i - m_j p_j\right)\,, \tag{6b}$$

where p_i is an auxiliary power variable and $k_i > 0$ is a gain, for each $i \in \mathcal{V}_I$. The matrix L is the Laplacian (or Kirchoff) matrix corresponding to a weighted, undirected and connected *communication graph* between the inverters, see Figure 1. The control architecture is depicted in Figure 3. The DAPI controller has the following three key properties:

(i) the controller is able to quickly regulate the network frequency under large and rapid variations in load,

(ii) the controller accomplishes this regulation while *preserving* the power sharing properties of the primary droop controller (2a) (see Section V), and

(iii) the communication network between the inverters need only be connected – we do not require all-to-all or all-to-one communication among the inverters (Figures 1 and 3).

While we omit a formal statement due to space, one can show that the secondary controller succeeds in restoring the network frequency and sharing power among the inverters if and only if the primary droop control stability condition (4). That is, the secondary control works if the primary control works, and vice versa [11].

A. Communication Complexity vs. Redundancy

The key feature of our control architecture is that it is *distributed*. That is, the inverters do not need to communicate information to a central microgrid controller. All that is required is that every inverter is able to at least *indirectly* communicate with every other inverter, see Figure 1. This distributed architecture for the cyber-physical layer of the controller allows for flexibility in the design. Specifically, one is able to trade off communication complexity against communication redundancy without impacting the functionality of the secondary control. While for mathematical simplicity, we have presented our theoretical results for the case of continuous time communication, all results extend to discrete time and asynchronous communication, see [22]. Moreover, it has been shown that secondary control strategies are generally robust against packet losses and delays, see [23]

VII. Experimental Results

Experiments were performed at Aalborg University in order to evaluate the performance of the DAPI controller (6a)–(6b). A schematic of the experimental setup is shown in Figure 4, in which two inverters operating in *parallel* supply power to a nonlinear load.

Figure 5 shows the experimental setup, which consisted of two Danfoss® 2.2 kW inverters operating at 10kHz with LCL output filters, a dSPACE® 1103 control board, and LEM® voltage and current sensors. A diode rectifier was used as a nonlinear load, loaded by a capacitor, and 200 Ω resistor. The electrical setup and control system parameters are detailed in Table I. Control parameters for both inverters were identical, and the inverter voltages were controlled according to the $E-Q$ droop method (2b) with $Q_i^* = 0$ for $i \in \{1, 2\}$.

Experimental results are shown in Figure 6. Figure 6 (a) shows the microgrid frequency being regulated to its nominal value by the DAPI controller. During the first two seconds of operation under only the droop controller (2a), a steady state frequency deviation exists. When the full DAPI controller is implemented at t=2s, the system frequency is successfully regulated. In the latter half of the experiment, the load was quickly varied twice: at t=9s (from 200Ω to 400Ω) and at t=14s (from 400Ω to 200Ω) respectively. As seen, the controller is able to quickly regulate the network frequency despite rapid load variation. For clarity, the secondary gains

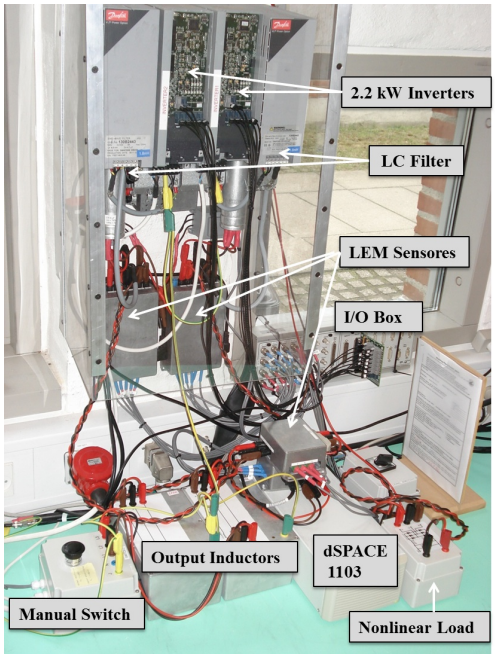

Fig. 5. Labeled diagram of experimental setup.

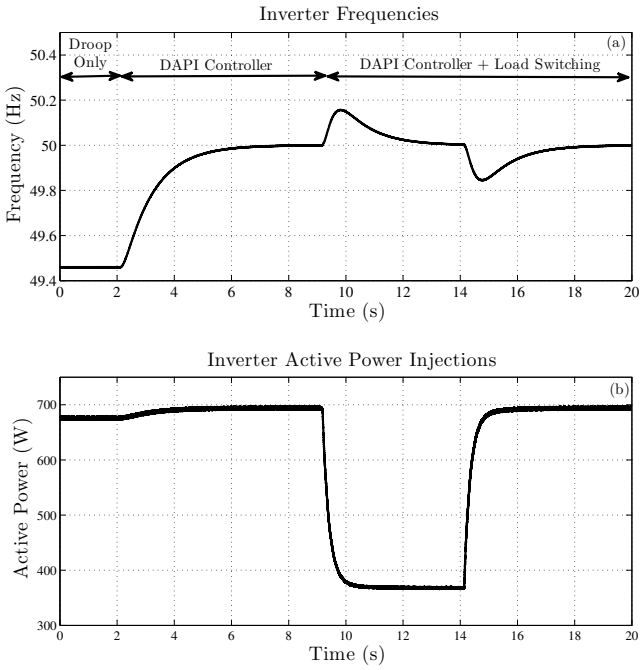

Fig. 6. Performance of DAPI Controller (6a)-(6b) for (a) frequency restoration, and (b) active power sharing.

k_i have been tuned so that the frequency restoration visible. The transient deviations in frequency caused by the load steps can be further suppressed, and their duration decreased, by decreasing k_i. Figure 6 (b) shows the corresponding active power injections at the inverters. This illustrates that the primary $P-\omega$ droop method is sufficient to share the active power accurately between the two inverters, and that the DAPI controller preserves the power sharing properties established by the primary controller. The small increase in active power at t=2s is due to the fact that the load is not a true constant power load, and indeed contains a frequency dependent component.

VIII. Simulation Extensions

To demonstrate the robustness of our approach in a large lossy network, in this section we present a simulation of our algorithm applied to the IEEE 37-bus distribution network (Figure 7). After an islanding event, the distribution network is disconnected from the larger transmission grid, and the distributed generators must taken action to ensure stability in the network while regulating the frequency and sharing both active and reactive loads. The cyber layer describing the communication capabilities of the distributed generators is shown in dotted blue.

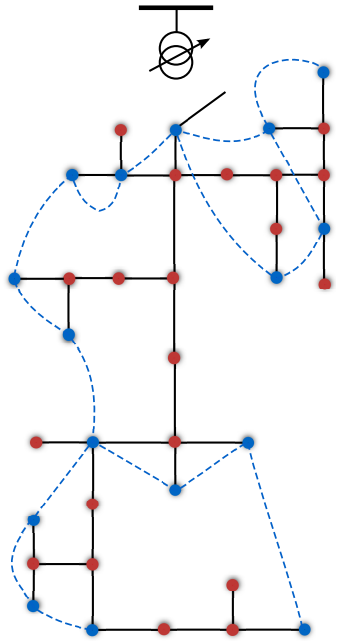

Fig. 7. Islanded IEEE37 bus distribution network. Red notes are strictly loads, while blue nodes represent distributed generation and load. The dotted blue lines represent communication links.

The DAPI controller (6a)–(6b) is used to regulate the $P-\omega$ dynamics in the network, while the $Q-E$ dynamics are governed by the *quadratic droop controller* [24]

$$\frac{\mathrm{d}}{\mathrm{d}t}E_i = -C_i E_i (E_i - E_i^*) - Q_i$$

along with an additional secondary control loop to ensure reactive power sharing. Figure 7 shows the performance of the algorithm, when one of the loads suddenly doubles at $t = 5$s. The controllers are seen to quickly restore the network frequency while maintaining exact sharing of active and reactive power demands in proportion to the respective capabilities of the generation.

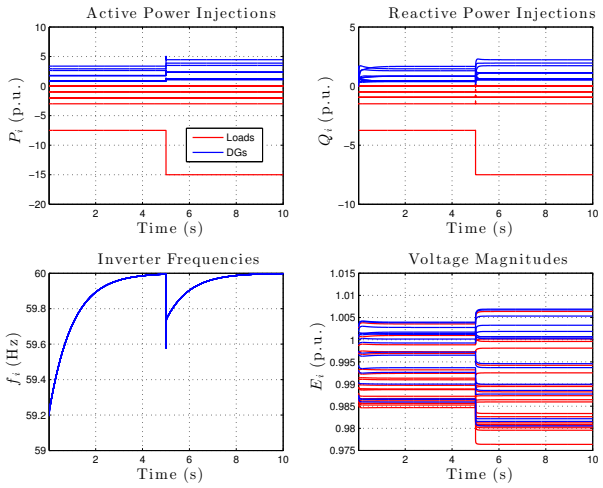

Fig. 8. Simulation results for IEEE37 bus distribution network.

TABLE I
PARAMETER VALUES FOR EXPERIMENTS.

Parameter	Symbol	Value
Electrical Setup		
Nom. Frequency	$\omega^*/2\pi$	50 Hz
DC Voltage	$V_{\rm dc}$	650 V
Nom. Voltages	E_i^*	311 V
Filter Capacitance	C	25 μF
Filter Inductance	L_f	1.8 mH
Output Impedance	L_0	1.8 mH
Resistive Load	$R_L(t)$	$R_L \in \{200, 400\}\Omega$
Inner Voltage/Current Control Loops		
Current Propor. Gain	k_{pi}	0.35 V/A
Current Integral Gain	k_{ii}	200 Vs/A
Voltage Propor. Gain	k_{pv}	0.35 A/V
Voltage Integral Gain	k_{iv}	400 As/V
DAPI Control		
Inv. Ratings (P)	Q_i^*	0 kvar
Inv. Ratings (Q)	$P_i^* = \overline{P}_i$	2.2 kW
$P-\omega$ Droop Coeff.	m_i	8×10^{-4} W $\cdot$ s/rad
$Q-E$ Droop Coef.	n_i	0.16 $\frac{\rm V}{\rm var}$
Sec. Droop Coeff.	k_i	1 s
Comm. Graph	$G_{\rm c}$	Two nodes, one edge
Comm. Weight	ℓ	1 Ws

IX. Conclusions

In this work we have surveyed our recent theoretical results on synchronization, power sharing, and secondary control in microgrids. In addition, we have presented experimental and simulation results validating our calculations. While throughout we have assumed inductive branches, in the case heavily mixed resistive/inductive lines, the primary control law (2a)–(2b) is inappropriate. A provably functional control strategy for general interconnections and line conditions is an open and exciting problem. Further work will examine provably robust controllers for mixed line networks, and how distributed control can be used to achieve additional goals such as harmonic compensation and fault tolerance.

References

[1] J. M. Guerrero, J. C. Vasquez, J. Matas, L. G. de Vicuna, and M. Castilla, "Hierarchical control of droop-controlled AC and DC microgrids–a general approach toward standardization," *IEEE Transactions on Industrial Electronics*, vol. 58, no. 1, pp. 158–172, 2011.

[2] J. A. P. Lopes, C. L. Moreira, and A. G. Madureira, "Defining control strategies for microgrids islanded operation," *IEEE Transactions on Power Systems*, vol. 21, no. 2, pp. 916–924, 2006.

[3] A. Tuladhar, H. Jin, T. Unger, and K. Mauch, "Parallel operation of single phase inverter modules with no control interconnections," in *Applied Power Electronics Conference and Exposition*, Atlanta, GA, USA, Feb. 1997, pp. 94–100.

[4] S. Barsali, M. Ceraolo, P. Pelacchi, and D. Poli, "Control techniques of dispersed generators to improve the continuity of electricity supply," in *IEEE Power Engineering Society Winter Meeting*, New York, NY, USA, Jan. 2002, pp. 789–794.

[5] R. Majumder, A. Ghosh, G. Ledwich, and F. Zare, "Power system stability and load sharing in distributed generation," in *Power System Technology and IEEE Power India Conference*, New Delhi, India, Oct. 2008, pp. 1–6.

[6] Y. U. Li and C.-N. Kao, "An accurate power control strategy for power-electronics-interfaced distributed generation units operating in a low-voltage multibus microgrid," *IEEE Transactions on Power Electronics*, vol. 24, no. 12, pp. 2977–2988, 2009.

[7] J. M. Guerrero, J. C. Vasquez, J. Matas, M. Castilla, and L. G. de Vicuna, "Control strategy for flexible microgrid based on parallel line-interactive UPS systems," *IEEE Transactions on Industrial Electronics*, vol. 56, no. 3, pp. 726–736, 2009.

[8] H. Bevrani, *Robust Power System Frequency Control*. Springer, 2009.

[9] M. C. Chandorkar, D. M. Divan, and R. Adapa, "Control of parallel connected inverters in standalone AC supply systems," *IEEE Transactions on Industry Applications*, vol. 29, no. 1, pp. 136–143, 1993.

[10] R. Lasseter and P. Piagi, "Providing premium power through distributed resources," in *Annual Hawaii Int. Conference on System Sciences*, Maui, HI, USA, Jan. 2000, pp. 4042–4051.

[11] J. W. Simpson-Porco, F. Dörfler, and F. Bullo, "Synchronization and power sharing for droop-controlled inverters in islanded microgrids," *Automatica*, Nov. 2012, to appear.

[12] L. O. Chua, C. A. Desoer, and E. S. Kuh, *Linear and Nonlinear Circuits*. McGraw-Hill, 1987.

[13] N. Biggs, "Algebraic potential theory on graphs," *Bulletin of the London Mathematical Society*, vol. 29, no. 6, pp. 641–683, 1997.

[14] E. C. Furtado, L. A. Aguirre, and L. A. B. Tôrres, "UPS parallel balanced operation without explicit estimation of reactive power – a simpler scheme," *IEEE Transactions on Circuits and Systems II: Express Briefs*, vol. 55, no. 10, pp. 1061–1065, 2008.

[15] Q.-C. Zhong and T. Hornik, *Control of Power Inverters in Renewable Energy and Smart Grid Integration*. Wiley-IEEE Press, 2013.

[16] B. W. Williams, *Power Electronics: Devices, Drivers, Applications and Passive Components*. McGraw-Hill, 1992.

[17] E. A. A. Coelho, P. C. Cortizo, and P. F. D. Garcia, "Small-signal stability for parallel-connected inverters in stand-alone AC supply systems," *IEEE Transactions on Industry Applications*, vol. 38, no. 2, pp. 533–542, 2002.

[18] M. Dai, M. N. Marwali, J.-W. Jung, and A. Keyhani, "Power flow control of a single distributed generation unit with nonlinear local load," in *IEEE Power Systems Conference and Exposition*, New York, USA, Oct. 2004, pp. 398–403.

[19] M. N. Marwali, J.-W. Jung, and A. Keyhani, "Stability analysis of load sharing control for distributed generation systems," *IEEE Transactions on Energy Conversion*, vol. 22, no. 3, pp. 737–745, 2007.

[20] Y. Mohamed and E. F. El-Saadany, "Adaptive decentralized droop controller to preserve power sharing stability of paralleled inverters in distributed generation microgrids," *IEEE Transactions on Power Electronics*, vol. 23, no. 6, pp. 2806–2816, 2008.

[21] Q.-C. Zhong, "Robust droop controller for accurate proportional load sharing among inverters operated in parallel," *IEEE Transactions on Industrial Electronics*, vol. 60, no. 4, pp. 1281–1290, 2013.

[22] F. Bullo, J. Cortés, and S. Martínez, *Distributed Control of Robotic Networks*. Princeton University Press, 2009.

[23] Q. Shafiee, J. C. Vasquez, and J. M. Guerrero, "Distributed secondary control for islanded microgrids - A networked control systems approach," in *Annual Conference on IEEE Industrial Electronics Society*, Montréal, Canada, Oct. 2012, pp. 5637–5642.

[24] J. W. Simpson-Porco, F. Dörfler, and F. Bullo, "Voltage stabilization in microgrids using quadratic droop control," in *IEEE Conf. on Decision and Control*, Florence, Italy, Dec. 2013, submitted.